



Safeguarding outdoor cultural heritage materials in an ever-changing troposphere: Challenges and new guidelines for artificial ageing test / Andrea Fumonmi, Erika Brattich, Elena Bernardi, Cristina Chiavari, Laura Tositti. - In: JOURNAL OF CULTURAL HERITAGE, - ISSN 1296-2074. - STAMPA. - 59:January-February(2023), pp: 190-201. [DOI: 10.1016/j.culher.2022.12.003](https://doi.org/10.1016/j.culher.2022.12.003)

## Alma Mater Studiorum Università di Bologna Archivio istituzionale della ricerca

Safeguarding outdoor cultural heritage materials in an ever-changing troposphere: Challenges and new guidelines for artificial ageing test

This is the final peer-reviewed author's accepted manuscript (postprint) of the following publication:

*Published Version:*

*Availability:*

This version is available at: <https://hdl.handle.net/11585/910757> since: 2023-04-26

*Published:*

DOI: <http://doi.org/10.1016/j.culher.2022.12.003>

*Terms of use:*

Some rights reserved. The terms and conditions for the reuse of this version of the manuscript are specified in the publishing policy. For all terms of use and more information see the publisher's website.

This item was downloaded from IRIS Università di Bologna (<https://cris.unibo.it/>).  
When citing, please refer to the published version.

(Article begins on next page)

This is the final peer-reviewed accepted manuscript of:

Timoncini, A., Brattich, E., Bernardi, E., Chiavari, C., Tositti, L.,  
*Safeguarding outdoor cultural heritage materials in an ever-changing  
troposphere: Challenges and new guidelines for artificial ageing test*,  
Journal of Cultural Heritage 59 (2023) 190-2012

The final published version is available online at:

<https://doi.org/10.1016/j.culher.2022.12.003>

Rights / License: CC-BY-NC-ND 4.0 license

(<http://creativecommons.org/licenses/by-nc-nd/4.0/>)

The terms and conditions for the reuse of this version of the manuscript are specified in the publishing policy. For all terms of use and more information see the publisher's website.

This item was downloaded from IRIS Università di Bologna (<https://cris.unibo.it/>)

**When citing, please refer to the published version.**

# **Safeguarding outdoor cultural heritage materials in an ever-changing troposphere: challenges and new guidelines for artificial ageing test**

Andrea Timoncini<sup>a</sup>, Erika Brattich<sup>b\*</sup>, Elena Bernardi<sup>c</sup>, Cristina Chiavari<sup>a</sup>, Laura Tositti<sup>d</sup>

<sup>a</sup> Department of Cultural Heritage, University of Bologna, Via degli Ariani 1, 48121 Ravenna, Italy,

<sup>b</sup> Department of Physics and Astronomy «Augusto Righi», University of Bologna, via Irnerio 46, 40126 Bologna, Italy,

<sup>c</sup> Department of Industrial Chemistry «Toso Montanari», University of Bologna, Viale del Risorgimento 4, 40136 Bologna, Italy,

<sup>d</sup> Department of Chemistry «Giacomo Ciamician», University of Bologna, Via Selmi 2, Bologna, University of Bologna.

\*Corresponding author [erika.brattich@unibo.it](mailto:erika.brattich@unibo.it)

**Keywords:** atmospheric depositions, trend analyses, accelerated ageing test, Cultural Heritage

## **Abstract**

Outdoor Cultural Heritage (CH) suffers severe damage due to the interaction among physical and chemical atmospheric factors. To study the mechanisms of degradation and to test the effectiveness of experimental protective treatments, accelerated ageing tests and artificial rains are widely used. In a scenario where climate and tropospheric composition are changing, the compositional variation of atmospheric deposition might strongly contribute to a gap between the results obtained in laboratory and real-world outdoor exposure. To reduce this gap, updated synthetic solutions, representative of changed deposition, seem necessary for material testing so to set up better conservative strategies.

This study provides new formulations of ageing solutions representative of changed deposition in southern Europe, obtained through the analysis of trends and sources of ions in atmospheric bulk depositions (1997-2019 period) collected in a highly polluted area (Po Valley, Italy).

## **1. Introduction**

Outdoor Cultural Heritage (CH) materials are prone to degradation processes due to direct exposure and interaction with physical, chemical, and biological factors, especially in polluted environments.

As a rule, atmospheric pollutants represent fundamental factors in CH conservation, owing to their role in accelerating and intensifying the natural weathering of outdoor materials [1–4]. Currently, climate change is seen as a new threat to CH, in addition to the previous ones; indeed, this makes the troposphere not only warmer but simultaneously more reactive also toward CH outdoor materials [5,6].

Atmospheric composition change is tightly connected with climate change [1,5,7,8], since pollutants and greenhouse gases are typically co-emitted and synergistically produced (see secondary aerosol and ozone both contributing to air quality and climate issues) in complex and reactive mixtures by a wide range of pollution sources. In addition, past and current technological developments together with the efforts spent on climate mitigation contribute in turn to modifications in atmospheric energy exchange mechanisms as well as chemical properties. In fact, these changes have an overall influence on acidity, oxidation capacity and reaction kinetics of the troposphere [5,8].

Specifically, climate change is affecting the mechanisms of decay altering temperature, precipitation patterns, wind circulation and atmospheric moisture [9].

Currently, climate change effects on CH involve hardly predictable hazards, owing to a tight association with latitude and locally highly variable environmental conditions [4]. According

to [4,6] climate change can have both direct and indirect effects. As direct effects of the temperature increase, thermoclastism risk is expected to increase in the Mediterranean region, as well as the freeze-thaw/frost damage in northern Europe.

The increase in atmospheric moisture together with precipitation pattern change is directly responsible for the dissolution and recrystallization of salts because of wetting and drying cycles, as well as for changes in corrosion rate. Moreover, the increase in both atmospheric moisture and precipitation promotes microbial proliferation and the kinetics of chemical and biochemical reactions resulting in an indirect influence on degradation mechanisms [6,10]. However, the impact of climate change is not always detrimental. Examples of beneficial effects of climate change on the increase in material stability include for instance the decrease in frost-related damage foreseen for most of Europe and the decrease in corrosion caused by the increase in the pH value of atmospheric depositions [4], while unpredictability might affect the degradation of organic materials [4,10]. An extensive overview of the effects of climate change on CH has been recently published including an extremely detailed and up-to-date classification of a wide range of cases/types of deterioration in this highly diversified field of CH materials [6].

These current alterations are especially important for airborne particulate matter and ozone [5] deemed as the most critical pollutants owing to their negative connections with health, environment and climate and whose complex tropospheric reactivity triggers degradation and corrosion of outdoor CH materials, including weathering for stones, corrosion for metals, leaching of the constituting K and Ca for medieval glass, while soiling appears on all types of cultural heritage materials [11,12]. From climate change simulations for the period April to September from 2000-2009 to 2040-2049 under the SRES A1B scenario (very rapid economic growth, low population growth and rapid introduction of new and more efficient technology), tropospheric ozone (both a powerful oxidant and a greenhouse gas) is expected to decrease over northern Europe, but to increase mostly in southern Europe

(latitude south of 50 °) [13]. As reported in [14], the PM10 concentration in the 2050s is expected to strongly decrease in the European area (-12%), while reduced changes are projected for the Mediterranean area (-1%). These changes result not only from the decreases in traffic and industrial emissions owing to technological improvement in the typical emission sources such as vehicular traffic and industries but also from mineral dust outbursts and wildfires which are expected to increase, so altering aerosol and precipitation composition and the mechanisms of ozone formation itself [14–17].

Besides, tropospheric warming is expected to increase ammonia emissions [18,19]. However, owing to the synergism among the chemically reactive species in the troposphere and to their overall non-linearity, the local effects are highly unpredictable, requiring steady monitoring and updates [5,20].

Concerning outdoor CH conservation, there is a wide agreement on the most important atmospheric pollutants affecting their decay: sulfur dioxide (SO<sub>2</sub>), nitrogen oxides (NO<sub>x</sub>), ozone (O<sub>3</sub>), ammonia (NH<sub>3</sub>) and airborne particulate (PM) [12,21]. All these pollutants, tightly connected to one another, mainly interact with CH materials via wet or dry depositions.

SO<sub>2</sub> is one of the most aggressive atmospheric pollutants because of its acidifying properties, especially for stone and metals [22]. For instance, it is responsible for: (i) stone decay via gypsum [10,21] and black crust formation with PM incorporation [23–25]; (ii) metal corrosion, usually enhanced by the presence of other pollutants [26,27]; (iii) glass decay [28,29]. A synergistic effect in the presence of ozone and NO<sub>2</sub> is reported [21], contributing to further hygroscopicity, acidification and oxidation processes.

NO<sub>x</sub> gets importance in CH degradation via its acidifying and oxidizing effects [30,31] being a precursor of nitric and nitrous acids, PM and ozone.

The damaging effects of acidifying pollutants as well as PM are enhanced by the oxidation capacities of the atmosphere, which is largely due to ozone, H<sub>2</sub>O<sub>2</sub>, OH and NO<sub>3</sub> radicals. These compounds, also in synergy with other pollutants [21,30,31], may directly damage

organic materials such as pigments, textiles, surface coating, plastic, and natural rubber [32].

PM impact on materials depends mainly on its acidity, hygroscopicity, amount of carbon content and in general on its highly complex chemical composition [2].

Ammonia is the main alkaline substance in the troposphere reacting with sulfuric and nitric acids, thus resulting in their neutralization through the formation of hygroscopic salts, such as  $(\text{NH}_4)_2\text{SO}_4$ ,  $\text{NH}_4\text{HSO}_4$  and  $\text{NH}_4\text{NO}_3$  as a function of their respective amounts [33–35]. The interaction between ammonia and CH materials shows indirect and direct effects [36,37]. Moreover,  $\text{NH}_3$  plays a relevant role in stone deterioration/conservation through ammonia-oxidizing microorganisms [38].

During the last decades, in Europe, efficient environmental policies (“Air Quality Framework Directive 96/62/EC”, “Ambient Air Quality Directive 2008/50/EC” and the “Ambient Air Quality Directive & daughter Directive 2004/107/EC” [39]) have been adopted to reduce atmospheric emissions. From 1990 to 2019,  $\text{SO}_x$  and  $\text{NO}_x$  emissions show the most sensitive reductions across the EU (92 % and 59 %, respectively), while  $\text{NH}_3$  emissions decreased by 28%, followed by a relatively stable trend [40].

These reductions resulted in declining concentrations of some of the main atmospheric pollutants at the European level [40].

These changes in atmospheric composition are producing a shift in deposition composition and intensity [41–43]. Several studies reported an increase in atmospheric deposition pH [44–49] especially in the south of Europe, resulting from the significant decrease in the precursor of acidifying compounds (sulfuric and nitric acids), and from climate change effects, as well as the concurrent increase of  $\text{NH}_3$  emission processes [18,19,50,51] and increasing frequency of alkaline events such as  $\text{CaCO}_3$  rich Saharan dust outburst across southern Europe, together with changes in the circulation pattern over the Mediterranean area [49]. This suggests that major acids and alkalis in the troposphere are reaching

equivalence, with a pH dominated by  $\text{CO}_2/\text{H}_2\text{CO}_3$  carbonate beyond the equilibrium level characterized by a rain pH of 5.6 for an unpolluted troposphere [44,52]. The increase in rainwater pH value over 5.6 units leads to the introduction of the term alkaline rainwater [18]. According to model simulations, non-sea salt sulphates are expected to decrease, while oxidized and reduced nitrogen deposition remain comparatively high, as discussed in [53]. These changes in deposition composition combined with climate change, also lead to an increase in extreme events in some parts of the world, affecting the whole range of CH materials exposed to outdoor conditions [54]. Specifically, precipitation is projected to increase in northern Europe, leading to a dilution of the rainwater ions, and to decrease in southern Europe, leading to a higher concentration of rainwater ions [55,56]. In the rainiest areas, this causes an increase in stone recession on marble and limestone [4], via the Karst effect [57], despite the decrease in the atmospheric acidifying compounds. Regarding the metals, it is expected higher and lowers atmospheric corrosion in inland Northern and Southern Europe, respectively. Moreover, in coastal areas corrosion is projected to increase because of stable chloride depositions and higher temperatures [30]. Historic stained glass will experience a minor decrease in corrosion over Europe with the most critical areas where higher temperatures and humidity occur [4].

The understanding of CH material decay, nowadays, is performed utilizing models [4] and, especially, through accelerated ageing tests which simulate ambient conditions, in order to develop degradation patterns comparable to the real environment [30,58–66]. Accelerated ageing tests are also used to evaluate the effectiveness of the protective treatments to be applied on outdoor CH. Among the most common ageing tests, those including continuous or alternate immersion, spray, or runoff conditions, frequently employ ageing solutions simulating acid rains. Indeed, most of them considered, as a reference, pH and compositions typical of acid rains at the end of the 20<sup>th</sup> /beginning of the 21<sup>st</sup> century [49,50,67]. In particular, the used solutions had simple (e.g., diluted  $\text{H}_2\text{SO}_4$ ,  $\text{HNO}_3$  or acetic acid) or



relatively complex (e.g., a mix of acids and salts) compositions, with a pH value varying from 3 to 4.5 [60–62,64,68,69]. In some cases, solutions at pH 5 were considered [60,70]. These artificial solutions [71] demonstrated to be effective ageing media to reproduce and to understand the past, but decreasingly so for the present decay pattern mechanisms, since progressively their composition risks to be less representative of future atmospheric deposition.

Based on the current changes in atmospheric composition and climate conditions previously described, the ageing tests need to be tailored and updated formulations of atmospheric deposition reflecting the current scenario, especially at the southern European level. These new formulations are expected to reduce gaps between degradation patterns obtained in the laboratory and those occurring in future real scenarios, so allowing the setting up of the most suitable conservation strategies, for any CH materials exposed to outdoor conditions.

## **2. Research aim**

The present study aims to provide a suitable range of ion concentrations to formulate representative solutions of the current atmospheric depositions especially for southern Europe, to be used in CH testing material. This is carried out by analyzing the trend and sources of ions in atmospheric bulk depositions collected in “Boschi di Carrega”, a typical southern European location in a highly polluted area, Po Valley, Italy.

The choice of the sampling location allows the application of our results to a wide variety of locations across Europe, especially in Southern Europe-Mediterranean, recognized as one of the most important global air pollution crossroads [72].

Indeed, the Po Valley represents one of the most environmentally and climatically vulnerable regions in Europe [72,73], characterized by both high air pollution levels and an increasingly significant marine aerosol input. Importantly, the Po Valley is also home to a great number of CH artefacts which are also UNESCO cultural sites [12]. As such, the updated ageing

solution will find connection and application to the current degradation and safeguarding of a wide variety of CH materials.

Finally, the results obtained from this trend analysis applied to the “Boschi di Carrega” site have been supported by data reported in other southern European sites. The studies we selected to support our findings are composed of other long-term data series collected in the Southern Europe-Mediterranean region, specifically in: Lake Maggiore, Italy [45], Granada, Spain [44], and various French sites [48]. Moreover, further confirmations on the currently increasing pH value come from [74].

The output of this study is updated formulations of synthetic ageing solution for CH material testing, representative of the changed current tropospheric composition caused by climate change and emission reductions obtained from trend analysis of rainwater composition from a robust and long-term time series of rainwater from 1997 to 2019.

### **3. Material and methods**

The data used for the present analysis were obtained from the Italian Conecofor/EMEP network operation (<http://www.enveurope.eu/partners/conecofor>) based on bulk depositions in different forest ecosystems, from May 1997 to December 2019, with a gap in 2017 and 2018 years.

The data chosen for the present work derive from samplings carried out by bulk precipitation collector in open field conditions, to minimize the influence of throughfall and stemflow deposition by tree canopy [51,75], and include pH, EC, alkalinity, and ions concentration, all determined according to the Conecofor protocols [75]. The ion speciation dataset (in mg/L) covers  $\text{Na}^+$ ,  $\text{NH}_4^+$ ,  $\text{K}^+$ ,  $\text{Mg}^{2+}$ ,  $\text{Ca}^{2+}$ ,  $\text{Cl}^-$ ,  $\text{NO}_3^-$ ,  $\text{SO}_4^{2-}$  and  $\text{PO}_4^{3-}$ . To analyse the temporal trend, monthly volume-weighted average alkalinity and ion concentrations were calculated from weekly data. Weekly pH data were converted into monthly data after conversion

into hydrogen ion molar concentration to prevent biases from the use of the logarithmic notation for pH.

Correlation and scatter plot analysis were performed to detect ion sources.

This has been performed in the “R” statistical environment [76], using the Ggally and ggplot2 packages [77].

The use of this dataset may show some limitations due to the type of sampler used because it samples both wet and dry deposition together with no possibility to distinguish between them. In addition, the bulk precipitation collector might also capture occult precipitation, i.e., fog, which besides being frequent in the cold season in this region, might represent an important degradation factor since it is generally more concentrated and with a lower pH than the common rainwater [78]. These aspects must be considered in the formulation process of synthetic atmospheric depositions. However, the advantages of choosing this site are linked to the length of the sampling period (20 years) and is representative of a background site in the Po Valley, one of the highest polluted areas of Europe and recognized as a hotspot of climate change [79].

### 3.1. Sampling site

Data elaborated in this work refers to the Conecofor sampling site (Fig. 1) located at Boschi di Carrega Regional Park (Cittadella - Sala Baganza, PR, Italy) at 200m a.s.l. in a typical oak forest (*Quercus petraea*) in the Po Valley. The climate in this area is characterized by bi-polar behaviour in precipitation patterns typical of the Mediterranean climate [47]. Indeed, maximum precipitation occurs in November (Autumn) and April (Spring) because of the strong influence of Genoa cyclogenesis, while minimum occurs during Winter and Summer [80]. At this location, the average annual rainfall is about 843 mm, while the average annual temperature is around 12.6 °C. Analyses of annual mean precipitation data in the region highlighted an overall decrease in rainfall (about 10-20% in 1961-2008) together with an increase in heavy precipitation events [81].

### 3.2. Trend analysis

Trend analysis on ions and on the  $\text{NH}_4^+/\text{NO}_3^-$  and  $\text{NH}_4^+/\text{SO}_4^{2-}$  ratios was carried out by means of two different non-parametric techniques, i.e., the Mann-Kendall (M-K) tau Test (MKT) and the Seasonal Mann Kendall Test; the magnitude of the trends was estimated by Theil-Sen (T-S) slope [82,83]. MKT is a test for monotonic trends [84]. The Seasonal Mann-Kendall Test instead applies the M-K trend test separately for each month and then combines the results [82,83,85]. Both tests are among the most widely used in the climatological analysis of precipitation, as documented by [86–90].

All trend analyses were performed in the “R” statistical environment using the “open air”, “trend”, “kendall”, “Ggally”, “ggplot2” and “zoo” packages [77]. The missing data in the 2017-2018 period have been replaced in the calculation. Specifically, missing values are replaced by linear interpolation via the “approx.” R function available through the “zoo” package.

## 4. Results and Discussion

Figure 2 shows the correlation between the sum of cations and anions to document the quality control of the data. A good correlation between anions and cations can be observed ( $R^2 = 0.72$ ), together with a deficit in anion contribution. This discrepancy can be attributed to the absence, in the balance, of carbonates/bicarbonates anions (unavailable in the ion chromatography dataset). They represent the typical counterions of  $\text{Ca}^{2+}$  and  $\text{Mg}^{2+}$  of environmental origin [47], which are relatively abundant in the processed dataset, with a mean concentration level of about  $68 \mu\text{eq/L}$ . This agrees with [47] and [91] who reported mean carbonate levels in the range of  $39\text{--}62 \mu\text{eq/L}$  in two different sites in the Po Valley.

### 4.1. General features of bulk deposition from open field sampling

Basic statistics of pH measured electrical conductivity (EC), cations and anions from bulk deposition samples during the period May 1997 to December 2019 are reported in Table 1. The mean and maximum values of EC (respectively  $21 \mu\text{S cm}$  and  $123 \mu\text{S cm}$ ) reveal the low ionic content of the collected samples. The mean EC value and its range agree with previous studies in other Mediterranean sites [44,47,92]. A wide range of variability in ion concentrations is observed over the sampling period. Indeed, the variation observed from the minimum to the maximum value is up to two orders of magnitude for all ions. Specifically, the parameters with the highest variability are  $\text{Na}^+$ ,  $\text{Ca}^{2+}$ ,  $\text{Cl}^-$ ,  $\text{PO}_4^{3-}$ ,  $\text{K}^+$  and pH. A huge variability is revealed by the difference between mean and median as well as between minimum and maximum values. This is likely associated with the variations in aerosol composition, in meteo-climatic conditions including precipitation amounts, in the past decades [93].

Subsequently we report the mean ion concentrations (in  $\mu\text{eq/L}$ ) in increasing order:

- Anions:  $\text{PO}_4^{3-}$  (0.25) <  $\text{NO}_3^-$  (11.5) <  $\text{Cl}^-$  (23.4) <  $\text{SO}_4^{2-}$  (40.5).

- Cations:  $K^+$  (4.5) <  $Mg^{2+}$  (10.8) <  $NH_4^+$  (52.4) <  $Ca^{2+}$  (56).

This dataset shows pH values ranging from 4.5 to 7.4 with both the average and the median value around 6 (Table 1). With a pH > 5.6, the deposition pH can be substantially classified as alkaline [94]. The neutralizing action is attributable to calcium carbonate and ammonia of crustal and agricultural origin respectively, in association with the high contribution of both  $Ca^{2+}$  and  $NH_4^+$  and in agreement with previous works [47,91,95]. Calcium carbonate and ammonia are currently recognized as the major neutralizing agents [86,93]. Carbonates/bicarbonates were estimated based on the sum of Ca and Mg, from the ionic balance and from alkalinity ([47] and references therein) leading to mean values of  $59.3 \pm 72.4 \mu\text{eq/L}$ ,  $68.5 \pm 62.4 \mu\text{eq/L}$  and  $51.9 \pm 70.1 \mu\text{eq/L}$  respectively. All the estimates are fairly similar to one another, though affected by high variability as previously reported [96]. Our data highlight a slight chlorine depletion ( $Cl^-/Na^+$  ratio is equal to  $(1.71 \pm 0.49) \text{ mg/L}$ , i.e., vs,  $(Cl^-/Na)_{\text{seawater}} = 1.795$ ).

Fig. 3 reports the scatterplot matrix between each couple of ions (in mg/L), together with their Spearman's rank correlation coefficient values (R) and frequency distribution. The significance level is indicated by the number of stars. Low correlation values ( $R < 0.4$ ) indicate the absence of linear correlation between the variables; R ranging between 0.4 and 0.7 suggests a certain degree of correlation though relatively complex. Lastly, high values of the correlation coefficient ( $R > 0.7$ ) indicate a large degree of association (covariance) between couples of variables. In this dataset, it is possible to observe only a few strong correlation values, and specifically between:  $SO_4^{2-}-NO_3^-$ ,  $NO_3^- - NH_4^+$ ;  $Na^+ - Cl^-$ ,  $Mg^{2+} - Na^+$ . The couples which show intermediate correlation are  $Ca^{2+} - Mg^{2+}$ ,  $Cl^- - Mg^{2+}$ ,  $SO_4^{2-} - Mg^{2+}$ ,  $NO_3^- - Mg^{2+}$ ,  $NH_4^+ - Mg^{2+}$ ,  $SO_4^{2-} - Ca^{2+}$ ,  $NO_3^- - Ca^{2+}$ ,  $SO_4^{2-} - Cl^-$ ,  $SO_4^{2-} - NH_4^+$ ,  $SO_4^{2-} - Na^+$ ,  $Mg^{2+} - K^+$ ,  $Ca^{2+} - K^+$ ,  $Na^+ - NO_3^-$ . These correlations are in agreement with the origin of the ions. In particular, the Secondary

Inorganic Aerosol, SIA ( $\text{SO}_4^{2-}$ ,  $\text{NO}_3^-$  and  $\text{NH}_4^+$ ), derives from the atmospheric processing of their gaseous precursors  $\text{SO}_2$  and  $\text{NO}_x$  [95,96].

The high correlation  $\text{Na}^+\text{-Cl}^-$  and between  $\text{Na}^+$  and  $\text{Mg}^{2+}$  reveal their common origin from marine aerosol [34]. Though  $\text{Ca}^{2+}$  and especially  $\text{Mg}^{2+}$  may partially derive from marine aerosol, they usually have a crustal origin. Therefore, the high correlation toward nitrates and sulfates can be explained by soil resuspension ( $\text{NO}_3^-$  vs.  $\text{Ca}$  and  $\text{Mg}^{2+}$ ) and/or the neutralization of  $\text{H}_2\text{SO}_4$  and  $\text{HNO}_3$  from atmospheric processing of  $\text{SO}_2$  and  $\text{NO}_x$  by  $\text{Ca}$  and  $\text{Mg}$  carbonates as typical aerosol components of crustal origin [30,95,97]. Finally, the pair  $\text{Mg}^{2+}\text{-K}^+$  may be explained by seasalt contribution, biomass burning and/or waste incineration [98].

#### **4.2. Seasonal pattern analysis**

Fig. 4 represents the monthly pattern of the main ions. Cations are shown in dashed line type and anions with a solid line type.  $\text{Ca}^{2+}$  shows high variability with a tendency to higher values from March to August, due to the higher aridity and consequent soil resuspension but including also the influence of Saharan dust outbreaks, as observed by [82]. It is to note that both seasalt and Saharan dust aerosols have been found to be efficient cloud condensation nuclei, therefore justifying the occurrence of the mentioned ions in precipitation and therefore in the bulk collectors. [79]. All the SIA derivatives increase in the winter precipitation as a result of different factors, increase in emission intensity, accumulation in the lower troposphere increased stability of  $\text{NH}_4\text{NO}_3$  at lower temperatures though the connection with precipitating clouds is never straightforward and given the circulation patterns in winter they might imply a contribution from transboundary pollution, since the Po Valley winter boundary layer though highly enriched in the airborne particulate matter has rarely the capacity of triggering precipitation owing to low-level stagnation [79].

Marine ions,  $\text{Na}^+$  and  $\text{Cl}^-$ , show higher values in autumn and winter, which may be due to the higher frequency of wind frontal situations coming from the Tyrrhenian Sea in autumn and winter [47,80].

### 4.3. Trend analysis

The trend analysis was applied to all the following variables (EC, pH, Alkalinity,  $\text{Na}^+$ ,  $\text{NH}_4^+$ ,  $\text{K}^+$ ,  $\text{Mg}^{2+}$ ,  $\text{Ca}^{2+}$ ,  $\text{Cl}^-$ ,  $\text{NO}_3^-$ ,  $\text{SO}_4^{2-}$ ,  $\text{PO}_4^{3-}$  as well as  $\text{NH}_4^+/\text{NO}_3^-$  and  $\text{NH}_4^+/\text{SO}_4^{2-}$  ratios), and results including trend and their significance are reported in Table 2. The ion ratios were included as they provide information about the degree of neutralization of nitric and sulfuric species by ammonia.

The results obtained reveal statistically significant trends especially using the Seasonal Kendall test rather than with Mann Kendall test. This suggests the presence of a strong seasonality within the time series in agreement with the local climatology, characterized by a bipolar precipitation pattern [47] and with the seasonal pattern previously shown in Fig. 3. Only chlorides and phosphate show less significant trends, while  $\text{NH}_4^+/\text{NO}_3^-$  ratio does not show any statistically significant trends. In table 2, also the mean change per year has been reported. This parameter indicates a slight decrease in the concentration of all parameters except for sulphate, which instead shows a more marked decline, and for the  $\text{NH}_4^+/\text{SO}_4^{2-}$  ratio, while pH shows an increasing trend, suggesting decreasing acidity. These observations are visually supported by the STL (Seasonal Trend decomposition based on Loess), which allows the decomposition and the estimation of the relative contributions of the seasonal, trend and residual components, reported in Fig. 5. Though some missing data in the 2017-2018 period might affect the analysis, the  $p$  significance levels of both Mann Kendall and the Seasonal Mann Kendall tests confirm the robustness of the emerging trends.



The observed highly significant upward trend in pH is in agreement with other studies and projections which seem to confirm this change in tropospheric chemistry across northern Italy and Europe in agreement with previous work [33,47–49,51,99]. The trend is shown in Fig. 5(a), where STL for pH is reported. The mean change of pH per year is +0.02. Considering the correlation analysis previously presented, acidity derived from H<sub>2</sub>SO<sub>4</sub> is mainly neutralized by gaseous ammonia but possibly by increasing contribution of mineral carbonates under the effect of increasing temperature and dry conditions as well as by increasing mineral dust contribution from the African desert. However, since the NH<sub>4</sub><sup>+</sup>/SO<sub>4</sub><sup>2-</sup> ratio shows an increase of 0.05 per year with high significance, given the tight stoichiometric connections between the two ions and the abundance of NH<sub>3</sub> (see further on in this paragraph) pH trend is mostly associated with the decrease in SO<sub>2</sub>-sulfates, namely in the H<sub>2</sub>SO<sub>4</sub> in connection with the well-known sulfur oxides emission/concentration as a result of the mitigation policy adopted in EU in the past decades. This is confirmed by the analysis of the trends in SO<sub>x</sub>, NO<sub>x</sub> and ammonia emissions at the European level. Indeed, the SO<sub>x</sub> emissions dropped by 92.2 % in the EU in the period 1990-2019, while in Italy the change was about 94% [40]. The decline of NO<sub>x</sub>, during the same period, was not as high as that for SO<sub>2</sub>, though NO<sub>x</sub> emissions have dropped by 58.8 % in the EU and of about 71% in Italy. Ammonia emissions, mainly due to agricultural activities, show a more limited decrease, only of 28.1 % in the EU and of about 24% in Italy. Regarding the concentration of SO<sub>2</sub>, it is still showing value above the EU daily threshold in 2 EU countries (Italy and Bulgaria), though a strong reduction was observed [73]. Our data reveal a mean pH value above 6 during the last decade with a median of 6.1 higher than the pH of clean air rain (pH 5.6) for the entire analysed period, suggesting instead the inception of an alkalizing trend resulting from an increasing role of alkaline minerals in atmospheric acid/base chemistry. Other studies reveal the tendency towards more alkaline atmospheric depositions: for instance, [34] which analysed the wet deposition from 2000 to 2017, revealed a mean pH of about

4.80 (4.19 to 5.82) at the European level, in line with other [49,92]. [44] reported rain pH values within 5.8–7.0 in a Spanish background EMEP station significantly influenced by Saharan events rich in  $\text{CaCO}_3$ .

The STL for sulphate is reported in Fig. 5(b). In this graph, the trend is strongly decreasing and highly significant as observed in Table 2. The reduction observed is the consequence of the application of European ambient air directives such as the EU Ambient Air Quality Directives (AAQDs) introduced from 1998 onwards as previously described.

The STL time series for  $\text{NO}_3^-$  is shown in Fig. 5(c). The trend, in this period, is slightly declining and significant (Table 2). Our results agree with those of [99,100] which stated a decrease in  $\text{NO}_3^-$  concentration in precipitation by about 23% during the 1990-2009 period. During 2002 and 2003, high values in nitrate concentration occurred especially during winter. This means that nitrogen oxides still play a significant role in SIA formation and in the associated acidification as reported also by the [34]; indeed, the annual limit value for nitrogen dioxide continues to be widely exceeded over Europe [101].

The trend of ammonium and of calcium ions show similar peaks around 2002-2003. In 2002-2003 the high ammonium values (Fig. 5d) could be related to the maximum ammonia emission reached during 2003 [40], while that of calcium to Sahara dust deposition with alkaline event, as reported by [49] and [46]. What's more 2003 was one of the warmest years recorded in the last decades, suggesting a potentially high influence of mineral dust rich in  $\text{CaCO}_3$ .

For both series, however, the trend is constant or slightly decreasing, at a high statistical significance level. Their decrease is lower than those of acidifying compounds ( $\text{NO}_3^-$  and  $\text{SO}_4^{2-}$ ), thus, as consequence, pH tends to increase.

The ammonium trend is supported by the ammonia trend from the EEA Report No 05/2021 [40] and by [18] indicating the absence of trends or slightly increasing trends for ammonia, especially during the last decade. This is principally the consequence of the application of

animal manure to the soil and to the inorganic N-fertilizers also including urea. The stable value for ammonium is reported also by [5].

#### **4.4. Translating environmental evidence into an updated testing paradigm**

The analyses so far performed clearly show how not only meteo-climatic, but also environmental conditions, have changed in terms of atmospheric composition in recent decades. This suggests the need to produce an updated framework of information in material science and, particularly in CH, since CH behaviour under the current atmospheric conditions will reflect these atmospheric changes. The same holds for testing and simulating conditions designed to assess mechanisms and patterns of material degradation, under controlled conditions. Based on our analysis considering a long-term (22 years) time series of chemical composition analysed in bulk deposition, this work specifically addresses the formulation of ageing solutions, ready to use in material testing, with properties representative of southern Europe in terms of current atmospheric composition and climatic parameters. To this aim, table S11 (available in the supplementary material) and Fig. 6 report updated compositional data for the most important chemical parameters of atmospheric deposition from the last 10 years obtained from our dataset, and supported by findings from other selected locations in the southern Europe-Mediterranean area [44,45,48]. We have selected the last decade's data frame as representative of the current alkaline rainwater pH range, enlightening the changed troposphere observed currently in southern Europe as opposed to the acid rain typical of the past [4,44,49].

Rainwater can be no longer considered as an acidic medium, but alkaline owing to a pH value in atmospheric deposition higher than 5.6; indeed, the data show a higher pH value. The alkalinisation is confirmed in agreement with [48] who show an increase in pH value of  $0.3 \pm 0.1$  pH unit over the period 1995-2007, in line with our findings showing an overall increase of about 0.44 pH units over the longer time interval 1997-2019.

The results of this study are widely comparable with other Mediterranean locations, as evidenced by the similar pH values of [44] and by the similar concentration range of other water-soluble compounds across southern and central Europe [74].

From the considerations and the trend analysis previously reported, the newly proposed formulation should account for the average composition observed, based on the trend estimate analysis of the chemical parameters presented in Table 2. Moreover, it should be adapted in consideration of the location simulation, in a range from the minimum to the maximum value of those proposed in Table SI1 (available in supplementary materials) per each chemical parameter. In detail, electrical conductivity shows an average of 16.1  $\mu\text{S}/\text{cm}$  with a decreasing trend, in line with [44] which shows an EC ranging from 15.4 to 32.1. For what concerns the conjugate base of the strong acidifying compounds ( $\text{H}_2\text{SO}_4$  and  $\text{HNO}_3$ ), their average values are 26.8  $\mu\text{eq}/\text{L}$  and 9.6  $\mu\text{eq}/\text{L}$ , respectively. Ammonium shows an average of 45.4  $\mu\text{eq}/\text{L}$ . Sea salt components ( $\text{Na}^+$  and  $\text{Cl}^-$ ) show an average concentration of 17.7  $\mu\text{eq}/\text{L}$  and 19.0  $\mu\text{eq}/\text{L}$ , respectively. The base cation components,  $\text{Ca}^{2+}$ ,  $\text{K}^+$  and  $\text{Mg}^{2+}$ , show an average of 41.3  $\mu\text{eq}/\text{L}$ , 3.9  $\mu\text{eq}/\text{L}$  and 9.5  $\mu\text{eq}/\text{L}$ , respectively. Our base cations concentrations are higher in respect of the sum of those found by [48] and [45] with  $24 \pm 14$   $\mu\text{eq}/\text{L}$  and 20-30  $\mu\text{eq}/\text{L}$  during the 2000-2014 period, respectively, but in line with those reported in [44] due to high alkalinity event frequency.

Since the optimal formulation needs to consider the trend estimation and the environment to be simulated, based on the performed trend analysis and supported by the results from [74], for nitrate and sulfate concentrations it is suggested to apply values not higher than the average. Actually, a mean change per year of 0.01 and -0.09  $\mu\text{eq}/\text{L}/\text{year}$  respectively was found, in line with [49] and with the future climate projections [53]. In the case of testing material behaviour in a simulated highly polluted area the maximum of their proposed values is suggested. At the same time, both ammonium and calcium, the most significant neutralizing compounds, show constant or slightly decreasing trends at most, in agreement

with [45,48]. For this reason, if the test wants to be representative of locations with high  $\text{NH}_4^+$  concentration, such as the Po Valley,  $\text{NH}_4^+$  values below the proposed averages should be avoided. Besides, it is important to consider the increasing importance of alkaline minerals such as  $\text{CaCO}_3$ , in agreement with the increasing trend of alkalizing episodes [45,48,49]. It is important to remark the positive trend for  $\text{NH}_4^+/\text{SO}_4^{2-}$  ratio and the constant trend for the  $\text{NH}_4^+/\text{NO}_3^-$  ratio, suggesting the currently reduced importance of  $\text{SO}_2$ . As for the sea salt component simulation, mainly consisting of  $\text{NaCl}$ , it is suggested to choose the maximum of the proposed values for coastal locations/areas, in order to maximize the conjunct effect of both anthropogenic and natural components.

The use of bulk rainwater dataset for this formulation may show some weaknesses. Indeed, the collected rainwater also includes dry deposition and soil resuspension. Therefore, the final analysed rainwater may result affected by higher pH and concentration because of the carbonates and salts presence. However, since the modus operandi of the artificial ageing test is aimed to stress the material with the extreme situation, these limitations can be viewed as possible strengths points because they may represent conditions close to the extreme one in Mediterranean areas, especially in the next decades.

## 5. Conclusions

This study provides updated ready-to-use ion concentrations for synthesising atmospheric deposition solutions to test materials in the context of climate change, specifically for southern European locations. To this aim, a long-term dataset (1997-2019) of the chemical composition of atmospheric bulk deposition collected in the Po Valley (Italy) was subjected to both source and trend analysis. The robustness of the analysis is provided by a large amount of data in the raw dataset (over 12 000 data) and by the significance of the correlation analysis obtained by two trend estimators (the Mann Kendall and Seasonal Mann Kendall Tests). Finally, the observed trends are supported by those emerging for bulk and

wet deposition at other Mediterranean locations. Our results indicate that atmospheric depositions are changing towards higher alkaline values, as pointed out by their pH mostly above 5.6 and characterized by a significant increasing trend. This results from the contemporary decreasing trends for sulphate and nitrate, together with the increasing importance of sub-Saharan input of carbonates and the stable ammonium concentration, in turn, due to global change. The herein proposed synthetic ageing solutions, to be used in material testing, reflect the compositional change in particular for the pH value increased, the reduced importance of sulfate and nitrate and, the alkalization provided by calcium, as well as by carbonates and ammonium.

### **Acknowledgements**

We wish to thank Aldo Marchetto (Consiglio Nazionale delle Ricerche-Istituto per lo Studio degli Ecosistemi) and also the CONECOFOR Network, the ICP IM and the programme ONU-ECE for the dataset provided. We also thank Pietro Morozzi (Department of Chemistry “G. Ciamician”, University of Bologna) for the support and suggestions in data analysis. We also wish to thank the R community, all contributors to the R packages used in this work, and ESRI and the GIS User Community for the map.

### **Funding**

This research did not receive any specific grant from funding agencies in the public, commercial, or not-for-profit sectors.

### **Data availability**

The raw/processed data required to reproduce these findings cannot be shared at this time as the data also forms part of an ongoing study.

## References

- [1] D. Camuffo, *Weathering of Building Materials*, (2016) 19–64. [https://doi.org/10.1142/9781783268863\\_0002](https://doi.org/10.1142/9781783268863_0002).
- [2] J. Watt, J. Tidblad, R. Hamilton, V. Kucera, *The effects of air pollution on cultural heritage*, Springer US, 2009. <https://doi.org/10.1007/978-0-387-84893-8>.
- [3] D. de la Fuente, J.M. Vega, F. Viejo, I. Díaz, M. Morcillo, Mapping air pollution effects on atmospheric degradation of cultural heritage, *J Cult Herit.* 14 (2013) 138–145. <https://doi.org/10.1016/j.culher.2012.05.002>.
- [4] C. Sabbioni, M. Cassar, P. Brimblecombe, *The atlas of climate change impact on European cultural heritage*, Anthem Press, London, 2010. <https://doi.org/10.2777/11959>.
- [5] P.S. Monks, C. Granier, S. Fuzzi, A. Stohl, M.L. Williams, H. Akimoto, M. Amann, A. Baklanov, U. Baltensperger, I. Bey, N. Blake, R.S. Blake, K. Carslaw, O.R. Cooper, F. Dentener, D. Fowler, E. Fragkou, G.J. Frost, S. Generoso, P. Ginoux, V. Grewe, A. Guenther, H.C. Hansson, S. Henne, J. Hjorth, A. Hofzumahaus, H. Huntrieser, I.S.A. Isaksen, M.E. Jenkin, J. Kaiser, M. Kanakidou, Z. Klimont, M. Kulmala, P. Laj, M.G. Lawrence, J.D. Lee, C. Liousse, M. Maione, G. McFiggans, A. Metzger, A. Mieville, N. Moussiopoulos, J.J. Orlando, C.D. O’Dowd, P.I. Palmer, D.D. Parrish, A. Petzold, U. Platt, U. Pöschl, A.S.H. Prévôt, C.E. Reeves, S. Reimann, Y. Rudich, K. Sellegri, R. Steinbrecher, D. Simpson, H. ten Brink, J. Theilake, G.R. van der Werf, R. Vautard, V. Vestreng, C. Vlachokostas, R. von Glasow, *Atmospheric composition change - global and regional air quality*, *Atmos Environ.* 43 (2009) 5268–5350. <https://doi.org/10.1016/j.atmosenv.2009.08.021>.
- [6] E. Sesana, A.S. Gagnon, C. Ciantelli, J.A. Cassar, J.J. Hughes, *Climate change impacts on cultural heritage: A literature review*, *Wiley Interdiscip Rev Clim Change.* 12 (2021) e710. <https://doi.org/10.1002/WCC.710>.
- [7] A. Groysman, *Corrosion in Natural and Industrial Environments, Corrosion for Everybody.* (2010) 109–150. [https://doi.org/10.1007/978-90-481-3477-9\\_3](https://doi.org/10.1007/978-90-481-3477-9_3).
- [8] E. von Schneidmesser, P.S. Monks, J.D. Allan, L. Bruhwiler, P. Forster, D. Fowler, A. Lauer, W.T. Morgan, P. Paasonen, M. Righi, K. Sindelarova, M.A. Sutton, *Chemistry and the Linkages between Air Quality and Climate Change*, *Chem Rev.* 115 (2015) 3856–3897. <https://doi.org/10.1021/acs.chemrev.5b00089>.
- [9] S. McCabe, D. Mcallister, C. Jamison, H.A. Viles, *A commentary on climate change, stone decay dynamics and the “greening” of natural stone buildings: New perspectives on “deep wetting” Reigate Stone at the Tower of London: Improving resilience in vulnerable historic masonry View project Cavernous features in sandstone View project*, *Article in Environmental Earth Sciences.* (2010). <https://doi.org/10.1007/s12665-010-0766-1>.
- [10] C.M. Grossi, P. Brimblecombe, I. Harris, *Predicting long term freeze-thaw risks on Europe built heritage and archaeological sites in a changing climate*, *Science of the Total Environment.* 377 (2007) 273–281. <https://doi.org/10.1016/j.scitotenv.2007.02.014>.
- [11] K. Vidović, · Samo Hočevar, · Eva Menart, I. Drventić, I. Grgić, A. Kroflič, *Impact of air pollution on outdoor cultural heritage objects and decoding the role of particulate matter: a critical review*, *Environmental Science and Pollution Research* 2022. 1 (2022) 1–33. <https://doi.org/10.1007/S11356-022-20309-8>.
- [12] P. Spezzano, *Mapping the susceptibility of UNESCO World Cultural Heritage sites in Europe to ambient (outdoor) air pollution*, *Science of the Total Environment.* 754 (2021). <https://doi.org/10.1016/j.scitotenv.2020.142345>.
- [13] J. Langner, M. Engardt, A. Baklanov, J.H. Christensen, M. Gauss, C. Geels, G.B. Hedegaard, R. Nuterman, D. Simpson, J. Soares, M. Sofiev, P. Wind, A. Zakey, *A multi-model study of*

- impacts of climate change on surface ozone in Europe, *Atmos Chem Phys*. 12 (2012) 10423–10440. <https://doi.org/10.5194/ACP-12-10423-2012>.
- [14] A. Cholakian, A. Colette, I. Coll, G. Ciarelli, M. Beekmann, Future climatic drivers and their effect on PM10 components in Europe and the Mediterranean Sea, *Atmos Chem Phys*. 19 (2019) 4459–4484. <https://doi.org/10.5194/acp-19-4459-2019>.
- [15] A. Colette, B. Bessagnet, R. Vautard, S. Szopa, S. Rao, S. Schucht, Z. Klimont, L. Menut, G. Clain, F. Meleux, G. Curci, L. Rouïl, European atmosphere in 2050, a regional air quality and climate perspective under CMIP5 scenarios, *Atmos Chem Phys*. 13 (2013) 7451–7471. <https://doi.org/10.5194/ACP-13-7451-2013>.
- [16] Y.F. Lam, J.S. Fu, S. Wu, L.J. Mickley, Impacts of future climate change and effects of biogenic emissions on surface ozone and particulate matter concentrations in the United States, *Atmos Chem Phys*. 11 (2011) 4789–4806. <https://doi.org/10.5194/ACP-11-4789-2011>.
- [17] B. Horemans, C. Cardell, L. Bencs, V. Kontozova-Deutsch, K. de Wael, R. van Grieken, Evaluation of airborne particles at the Alhambra monument in Granada, Spain, *Microchemical Journal*. 99 (2011) 429–438. <https://doi.org/10.1016/J.MICROC.2011.06.018>.
- [18] M.A. Sutton, N. van Dijk, P.E. Levy, M.R. Jones, I.D. Leith, L.J. Sheppard, S. Leeson, Y. Sim Tang, A. Stephens, C.F. Braban, U. Dragosits, C.M. Howard, M. Vieno, D. Fowler, P. Corbett, M.I. Naikoo, S. Munzi, C.J. Ellis, S. Chatterjee, C.E. Steadman, A. Móríng, P.A. Wolseley, Alkaline air: changing perspectives on nitrogen and air pollution in an ammonia-rich world: Alkaline Air, *Philosophical Transactions of the Royal Society A: Mathematical, Physical and Engineering Sciences*. 378 (2020). <https://doi.org/10.1098/rsta.2019.0315>.
- [19] M.A. Sutton, S. Reis, S.N. Riddick, U. Dragosits, E. Nemitz, M.R. Theobald, Y.S. Tang, C.F. Braban, M. Vieno, A.J. Dore, R.F. Mitchell, S. Wanless, F. Daunt, D. Fowler, T.D. Blackall, C. Milford, C.R. Flechard, B. Loubet, R. Massad, P. Cellier, E. Personne, P.F. Coheur, L. Clarisse, M. van Damme, Y. Ngadi, C. Clerbaux, C.A. Skjøth, C. Geels, O. Hertel, R.J.W. Kruit, R.W. Pinder, J.O. Bash, J.T. Walker, D. Simpson, L. Horváth, T.H. Misselbrook, A. Bleeker, F. Dentener, W. de Vries, Towards a climate-dependent paradigm of ammonia emission and deposition, *Philosophical Transactions of the Royal Society B: Biological Sciences*. 368 (2013). <https://doi.org/10.1098/RSTB.2013.0166>.
- [20] P.S. Monks, Gas-phase radical chemistry in the troposphere, *Chem Soc Rev*. 34 (2005) 376–395. <https://doi.org/10.1039/B307982C>.
- [21] F. Vidal, R. Vicente, J. Mendes Silva, Review of environmental and air pollution impacts on built heritage: 10 questions on corrosion and soiling effects for urban intervention, *J Cult Herit*. 37 (2019) 273–295. <https://doi.org/10.1016/j.culher.2018.11.006>.
- [22] P. Brimblecombe, The Effects of Air Pollution on the Built Environment, 2 (2003). <https://doi.org/10.1142/P243>.
- [23] P. Ausset, M. del Monte, R.A. Lefèvre, Embryonic sulphated black crusts on carbonate rocks in atmospheric simulation chamber and in the field: role of carbonaceous fly-ash, *Atmos Environ*. 33 (1999) 1525–1534. [https://doi.org/10.1016/S1352-2310\(98\)00399-9](https://doi.org/10.1016/S1352-2310(98)00399-9).
- [24] D. Camuffo, M. del Monte, C. Sabbioni, Origin and growth mechanisms of the sulfated crusts on urban limestone, *Water, Air, and Soil Pollution* 1983 19:4. 19 (1983) 351–359. <https://doi.org/10.1007/BF00159596>.
- [25] C.A. Price, G.G. Amoroso, V. Fassina, Stone Decay and Conservation: Atmospheric Pollution, Cleaning, Consolidation and Protection, *Studies in Conservation*. 29 (1984) 158. <https://doi.org/10.2307/1506020>.
- [26] J. Tidblad, K. Hicks, J. Kuylenstierna, B.B. Pradhan, P. Dangol, I. Mylvakanam, S.B. Feresu, C. Lungu, Atmospheric corrosion effects of air pollution on materials and cultural property in Kathmandu, Nepal, *Materials and Corrosion*. 67 (2016) 170–175. <https://doi.org/10.1002/MACO.201408043>.



- [27] S. Oesch, M. Faller, Environmental effects on materials: The effect of the air pollutants SO<sub>2</sub>, NO<sub>2</sub>, NO and O<sub>3</sub> on the corrosion of copper, zinc and aluminium. A short literature survey and results of laboratory exposures, *Corros Sci.* 39 (1997) 1505–1530. [https://doi.org/10.1016/S0010-938X\(97\)00047-4](https://doi.org/10.1016/S0010-938X(97)00047-4).
- [28] B. Messiga, M.P. Riccardi, Alteration behaviour of glass panes from the medieval Pavia Charterhouse (Italy), *J Cult Herit.* 7 (2006) 334–338. <https://doi.org/10.1016/j.culher.2006.03.004>.
- [29] M. Melcher, R. Wiesinger, M. Schreiner, Degradation of glass artifacts: Application of modern surface analytical techniques, *Acc Chem Res.* 43 (2010) 916–926. <https://doi.org/10.1021/ar9002009>.
- [30] J. Tidblad, Atmospheric corrosion of metals in 2010-2039 and 2070-2099, *Atmos Environ.* 55 (2012) 1–6. <https://doi.org/10.1016/j.atmosenv.2012.02.081>.
- [31] V. Kucera, S. Fitz, Direct and indirect air pollution effects on materials including cultural monuments, *Water, Air, and Soil Pollution* 1995 85:1. 85 (1995) 153–165. <https://doi.org/10.1007/BF00483697>.
- [32] A. Screpanti, A. de Marco, Corrosion on cultural heritage buildings in Italy: A role for ozone?, *Environmental Pollution.* 157 (2009) 1513–1520. <https://doi.org/10.1016/j.envpol.2008.09.046>.
- [33] R. Vet, R.S. Artz, S. Carou, M. Shaw, C.U. Ro, W. Aas, A. Baker, V.C. Bowersox, F. Dentener, C. Galy-Lacaux, A. Hou, J.J. Pienaar, R. Gillett, M.C. Forti, S. Gromov, H. Hara, T. Khodzher, N.M. Mahowald, S. Nickovic, P.S.P. Rao, N.W. Reid, A global assessment of precipitation chemistry and deposition of sulfur, nitrogen, sea salt, base cations, organic acids, acidity and pH, and phosphorus, *Atmos Environ.* 93 (2014) 3–100. <https://doi.org/10.1016/j.atmosenv.2013.10.060>.
- [34] Á. Keresztesi, M.V. Birsan, I.A. Nita, Z. Bodor, R. Szép, Assessing the neutralisation, wet deposition and source contributions of the precipitation chemistry over Europe during 2000–2017, *Environ Sci Eur.* 31 (2019). <https://doi.org/10.1186/s12302-019-0234-9>.
- [35] J.H. Seinfeld, S.N. Pandis, *Atmospheric Chemistry and Physics: From Air Pollution to Climate Change.*, Wiley & Sons, Inc., Hoboken, New Jersey USA, Third Edition. New Jersey USA, (2016) 1152. <http://vlib.kmu.ac.ir/kmu/handle/kmu/82106> (accessed January 18, 2022).
- [36] H. Bassett, R.G. Durrant, CCCXVII.—Action of ammonium nitrate and of aqueous ammonia on copper. Properties of cupric tetrammine nitrite and nitrate, *Journal of the Chemical Society, Transactions.* 121 (1922) 2630–2640. <https://doi.org/10.1039/CT9222102630>.
- [37] R. Francis, Effect of pollutants on corrosion of copper alloys in sea water: Part 1: Ammonia and chlorine, <http://Dx.Doi.Org/10.1179/000705985798272650>. 20 (2013) 167–174. <https://doi.org/10.1179/000705985798272650>.
- [38] H. Meng, Y. Katayama, J.D. Gu, More wide occurrence and dominance of ammonia-oxidizing archaea than bacteria at three Angkor sandstone temples of Bayon, Phnom Krom and Wat Athvea in Cambodia, *Int Biodeterior Biodegradation.* 117 (2017) 78–88. <https://doi.org/10.1016/J.IBIOD.2016.11.012>.
- [39] K. Kuklinska, L. Wolska, J. Namiesnik, Air quality policy in the U.S. and the EU - A review, *Atmos Pollut Res.* 6 (2015) 129–137. <https://doi.org/10.5094/APR.2015.015>.
- [40] European Environmental Agency, European Union emission inventory report 1990-2019 under the UNECE Convention on Long-range Transboundary Air Pollution (Air Convention), 2021. <https://doi.org/10.2800/701303>.
- [41] T. Grøntoft, Historical dry deposition of air pollution in the urban background in Oslo, Norway, compared to Western European data, *Atmos Environ.* 267 (2021) 118777. <https://doi.org/10.1016/J.ATMOSENV.2021.118777>.
- [42] R. Garaga, S. Chakraborty, H. Zhang, S. Gokhale, Q. Xue, S.H. Kota, Influence of anthropogenic emissions on wet deposition of pollutants and rainwater acidity in Guwahati, a

- UNESCO heritage city in Northeast India, *Atmos Res.* 232 (2020).  
<https://doi.org/10.1016/J.ATMOSRES.2019.104683>.
- [43] C.-H.M. Tso, D. Monteith, T. Scott, H. Watson, B. Dodd, M.G. Pereira, P. Henrys, M. Hollaway, S. Rennie, A. Lowther, J. Watkins, R. Killick, G. Blair, The evolving role of weather types on rainfall chemistry under large reductions in pollutant emissions, *Environmental Pollution*. 299 (2022) 118905.  
<https://doi.org/10.1016/J.ENVPOL.2022.118905>.
- [44] A.I. Calvo, F.J. Olmo, H. Lyamani, L. Alados-Arboledas, A. Castro, M. Fernández-Raga, R. Fraile, Chemical composition of wet precipitation at the background EMEP station in Víznar (Granada, Spain) (2002-2006), *Atmos Res.* 96 (2010) 408–420.  
<https://doi.org/10.1016/j.atmosres.2010.01.013>.
- [45] M. Rogora, L. Colombo, A. Marchetto, R. Mosello, S. Steingruber, Temporal and spatial patterns in the chemistry of wet deposition in Southern Alps, *Atmos Environ.* 146 (2016) 44–54. <https://doi.org/10.1016/j.atmosenv.2016.06.025>.
- [46] M. Rogora, R. Mosello, S. Arisci, M.C. Brizzio, A. Barbieri, R. Balestrini, P. Waldner, M. Schmitt, M. Stähli, A. Thimonier, M. Kalina, H. Puxbaum, U. Nickus, E. Ulrich, A. Probst, An overview of atmospheric deposition chemistry over the Alps: Present status and long-term trends, *Hydrobiologia*. 562 (2006) 17–40. <https://doi.org/10.1007/s10750-005-1803-z>.
- [47] L. Tositti, L. Pieri, E. Brattich, S. Parmeggiani, F. Ventura, Chemical characteristics of atmospheric bulk deposition in a semi-rural area of the Po Valley (Italy), *J Atmos Chem.* 75 (2018) 97–121. <https://doi.org/10.1007/s10874-017-9365-9>.
- [48] A. Pascaud, S. Sauvage, P. Coddeville, M. Nicolas, L. Croisé, A. Mezdour, A. Probst, Contrasted spatial and long-term trends in precipitation chemistry and deposition fluxes at rural stations in France, *Atmos Environ.* 146 (2016) 28–43.  
<https://doi.org/10.1016/j.atmosenv.2016.05.019>.
- [49] M. Rogora, R. Mosello, A. Marchetto, Long-term trends in the chemistry of atmospheric deposition in Northwestern Italy: the role of increasing Saharan dust deposition, *Tellus B: Chemical and Physical Meteorology*. 56 (2004) 426–434.  
<https://doi.org/10.3402/TELLUSB.V56I5.16456>.
- [50] L. Morselli, E. Bernardi, I. Vassura, F. Passarini, E. Tesini, Chemical composition of wet and dry atmospheric depositions in an urban environment: Local, regional and long-range influences, *J Atmos Chem.* 59 (2008) 151–170. <https://doi.org/10.1007/S10874-008-9099-9>.
- [51] A. Marchetto, A. Marchetto, S. Arisci, C. Brizzio, R. Mosello, G.A. Tartari, Status and trend of atmospheric deposition chemistry at the CONECOFOR plots, 1998-2005, *Annals of Silvicultural Research*. 34 (2013) 57–66. <https://doi.org/10.12899/asr-903>.
- [52] G.E. Likens, C.T. Driscoll, D.C. Buso, Long-Term Effects of Acid Rain: Response and Recovery of a Forest Ecosystem, *Science* (1979). 272 (1996) 244–246.  
<https://doi.org/10.1126/SCIENCE.272.5259.244>.
- [53] M. Engardt, D. Simpson, M. Schwikowski, L. Granat, Deposition of sulphur and nitrogen in Europe 1900–2050. Model calculations and comparison to historical observations, *Tellus B Chem Phys Meteorol.* 69 (2017). <https://doi.org/10.1080/16000889.2017.1328945>.
- [54] R.K. Pachauri, M.R. Allen, V.R. Barros, J. Broome, W. Cramer, R. Christ, J.A. Church, L. Clarke, Q. Dahe, P. Dasgupta, N.K. Dubash, O. Edenhofer, I. Elgizouli, C.B. Field, P. Forster, P. Friedlingstein, J. Fuglestedt, L. Gomez-Echeverri, S. Hallegatte, G. Hegerl, M. Howden, K. Jiang, B. Jimenez Cisneroz, V. Kattsov, H. Lee, K.J. Mach, J. Marotzke, M.D. Mastrandrea, L. Meyer, J. Minx, Y. Mulugetta, K. O'Brien, M. Oppenheimer, J.J. Pereira, R. Pichs-Madruga, G.-K. Plattner, H.-O. Pörtner, S.B. Power, B. Preston, N.H. Ravindranath, A. Reisinger, K. Riahi, M. Rusticucci, R. Scholes, K. Seyboth, Y. Sokona, R. Stavins, T.F. Stocker, P. Tschakert, D. van Vuuren, J.-P. van Ypserle, *Climate Change 2014: Synthesis Report. Contribution of Working Groups I, II and III to the Fifth Assessment Report of the Intergovernmental Panel on Climate Change, EPIC3* Geneva, Switzerland, IPCC, 151 p., Pp.

- 151, ISBN: 978-92-9169-143-2. (2014). [https://www.ipcc.ch/pdf/assessment-report/ar5/syr/SYR\\_AR5\\_FINAL\\_full\\_wcover.pdf](https://www.ipcc.ch/pdf/assessment-report/ar5/syr/SYR_AR5_FINAL_full_wcover.pdf) (accessed January 18, 2022).
- [55] S. Gualdi, S. Somot, L. Li, V. Artale, M. Adani, A. Bellucci, A. Braun, S. Calmanti, A. Carillo, A. Dell'Aquila, M. Déqué, C. Dubois, A. Elizalde, A. Harzallah, D. Jacob, B. L'Hévéder, W. May, P. Oddo, P. Ruti, A. Sanna, G. Sannino, E. Scoccimarro, F. Sevault, A. Navarra, The CIRCE Simulations: Regional Climate Change Projections with Realistic Representation of the Mediterranean Sea, *Bull Am Meteorol Soc.* 94 (2013) 65–81. <https://doi.org/10.1175/BAMS-D-11-00136.1>.
- [56] M. Reale, W.D. Cabos Narvaez, L. Cavicchia, D. Conte, E. Coppola, E. Flaounas, F. Giorgi, S. Gualdi, A. Hochman, L. Li, P. Lionello, Z. Podrascanin, S. Salon, E. Sanchez-Gomez, E. Scoccimarro, D. v. Sein, S. Somot, Future projections of Mediterranean cyclone characteristics using the Med-CORDEX ensemble of coupled regional climate system models, *Clim Dyn.* 1 (2021) 1–24. <https://doi.org/10.1007/S00382-021-06018-X/FIGURES/12>.
- [57] F.W. Lipfert, Atmospheric damage to calcareous stones: Comparison and reconciliation of recent experimental findings, *Atmospheric Environment* (1967). 23 (1989) 415–429. [https://doi.org/10.1016/0004-6981\(89\)90587-8](https://doi.org/10.1016/0004-6981(89)90587-8).
- [58] G. Masi, J. Esvan, C. Josse, C. Chiavari, E. Bernardi, C. Martini, M.C. Bignozzi, N. Gartner, T. Kosec, L. Robbiola, Characterization of typical patinas simulating bronze corrosion in outdoor conditions, *Mater Chem Phys.* 200 (2017) 308–321. <https://doi.org/10.1016/j.matchemphys.2017.07.091>.
- [59] C. Chiavari, E. Bernardi, A. Balbo, C. Monticelli, S. Raffo, M.C. Bignozzi, C. Martini, Atmospheric corrosion of fire-gilded bronze: Corrosion and corrosion protection during accelerated ageing tests, *Corros Sci.* 100 (2015) 435–447. <https://doi.org/10.1016/j.corsci.2015.08.013>.
- [60] E. Franzoni, E. Sassoni, Correlation between microstructural characteristics and weight loss of natural stones exposed to simulated acid rain, *Sci Total Environ.* 412–413 (2011) 278–285. <https://doi.org/10.1016/J.SCITOTENV.2011.09.080>.
- [61] C. Chiavari, E. Bernardi, C. Martini, F. Passarini, F. Ospitali, L. Robbiola, The atmospheric corrosion of quaternary bronzes: The action of stagnant rain water, *Corros Sci.* 52 (2010) 3002–3010. <https://doi.org/10.1016/j.corsci.2010.05.013>.
- [62] E. Bernardi, C. Chiavari, B. Lenza, C. Martini, L. Morselli, F. Ospitali, L. Robbiola, The atmospheric corrosion of quaternary bronzes: The leaching action of acid rain, *Corros Sci.* 51 (2009) 159–170. <https://doi.org/10.1016/j.corsci.2008.10.008>.
- [63] F. Samie, J. Tidblad, V. Kucera, C. Leygraf, Atmospheric corrosion effects of HNO<sub>3</sub>-Comparison of laboratory-exposed copper, zinc and carbon steel, *Atmos Environ.* 41 (2007) 4888–4896. <https://doi.org/10.1016/j.atmosenv.2007.02.007>.
- [64] L. Tecer, Laboratory Experiments on the Investigation of the Effects of Sulphuric Acid on the Deterioration of Carbonate Stones and Surface Corrosion, *Water, Air, and Soil Pollution* 1999 114:1. 114 (1999) 1–12. <https://doi.org/10.1023/A:1005177201808>.
- [65] J. Tidblad, C. Leygraf, Atmospheric Corrosion Effects of SO<sub>2</sub> and NO<sub>2</sub>: A Comparison of Laboratory and Field-Exposed Copper, *J Electrochem Soc.* 142 (1995) 749–756. <https://doi.org/10.1149/1.2048529/XML>.
- [66] L. Gianni, M. Cavallini, S. Natali, A. Adriaens, Wet and Dry Accelerated Aging Tests in a Spray Chamber to Understand the Effects of Acid Rain Frequencies on Bronze Corrosion, *Int. J. Electrochem. Sci.* 8 (2013) 1822–1838.
- [67] L. Morselli, E. Bernardi, C. Chiavari, G. Brunoro, Corrosion of 85-5-5-5 bronze in natural and synthetic acid rain, *Appl Phys A Mater Sci Process.* 79 (2004) 363–367. <https://doi.org/10.1007/S00339-004-2536-Y>.
- [68] A. Misra, I. Franco Castillo, D.P. Müller, C. González, S. Eyssautier-Chuine, A. Ziegler, J.M. de la Fuente, S.G. Mitchell, C. Streb, Polyoxometalate-Ionic Liquids (POM-ILs) as

- Anticorrosion and Antibacterial Coatings for Natural Stones, *Angew Chem Int Ed Engl.* 57 (2018) 14926–14931. <https://doi.org/10.1002/ANIE.201809893>.
- [69] L. Gianni, G.E. Gigante, M. Cavallini, A. Adriaens, Corrosion of Bronzes by Extended Wetting with Single versus Mixed Acidic Pollutants, *Materials (Basel)*. 7 (2014) 3353–3370. <https://doi.org/10.3390/MA7053353>.
- [70] S. Gibeaux, P. Vázquez, T. de Kock, V. Cnudde, C. Thomachot-Schneider, Weathering assessment under X-ray tomography of building stones exposed to acid atmospheres at current pollution rate, *Constr Build Mater.* 168 (2018) 187–198. <https://doi.org/10.1016/J.CONBUILDMAT.2018.02.120>.
- [71] W. He, I. Odnevall Wallinder, C. Leygraf, A laboratory study of copper and zinc runoff during first flush and steady-state conditions, *Corros Sci.* 43 (2001) 127–146. [https://doi.org/10.1016/S0010-938X\(00\)00066-4](https://doi.org/10.1016/S0010-938X(00)00066-4).
- [72] J. Lelieveld, H. Berresheim, S. Borrmann, P.J. Crutzen, F.J. Dentener, H. Fischer, J. Feichter, P.J. Flatau, J. Heland, R. Holzinger, R. Kormann, M.G. Lawrence, Z. Levin, K.M. Markowicz, N. Mihalopoulos, A. Minikin, V. Ramanathan, M. de Reus, G.J. Roelofs, H.A. Scheeren, J. Sciare, H. Schlager, M. Schultz, P. Siegmund, B. Steil, E.G. Stephanou, P. Stier, M. Traub, C. Warneke, J. Williams, H. Ziereis, Global air pollution crossroads over the Mediterranean, *Science* (1979). 298 (2002) 794–799. <https://doi.org/10.1126/SCIENCE.1075457>.
- [73] European Environment Agency., Air quality in Europe-2020 report. No 09/2020, 2020.
- [74] Terje Grøntoft, Marta Segura Roux, NILU Report No 02/2020: Convention on long-range transboundary air pollution. UN/ECE international co-operative programme on effects on materials, including historic and cultural monuments. Environmental data report. October 2017 to November 2018., 2020.
- [75] A. Marchetto, S. Arisci, G. Tartari, R. Balestrini, D. Tait, Current state and temporal evolution of the chemical composition of atmospheric depositions in forest areas of the CONECOFOR network, *Forest@ - Rivista Di Selvicoltura Ed Ecologia Forestale*. 11 (2014) 72–85. <https://doi.org/10.3832/efor1003-011>.
- [76] R Development Core Team. R A Language and Environment for Statistical Computing. R Foundation for Statistical Computing, Vienna, Austria. R Foundation for Statistical Computing, Vienna. - References - Scientific Research Publishing, (2014). [https://www.scirp.org/\(S\(i43dyn45teexjx455qlt3d2q\)\)/reference/ReferencesPapers.aspx?ReferenceID=1622068](https://www.scirp.org/(S(i43dyn45teexjx455qlt3d2q))/reference/ReferencesPapers.aspx?ReferenceID=1622068) (accessed July 4, 2022).
- [77] D.R. Helsel, L.M. Frans, Regional Kendall test for trend, *Environ Sci Technol.* 40 (2006) 4066–4073. <https://doi.org/10.1021/ES051650B>.
- [78] L. Giulianelli, S. Gilardoni, L. Tarozzi, M. Rinaldi, S. Decesari, C. Carbone, M.C. Facchini, S. Fuzzi, Fog occurrence and chemical composition in the Po valley over the last twenty years, *Atmos Environ.* 98 (2014) 394–401. <https://doi.org/10.1016/J.ATMOSENV.2014.08.080>.
- [79] S. Finardi, C. Silibello, A. D’Allura, P. Radice, Analysis of pollutants exchange between the Po Valley and the surrounding European region, *Urban Clim.* 10 (2014) 682–702. <https://doi.org/10.1016/j.uclim.2014.02.002>.
- [80] M. Hulme, E. Barrow, *Climates of the British Isles : present, past, and future*, Routledge, 1997.
- [81] S. Persiano, E. Ferri, G. Antolini, A. Domeneghetti, V. Pavan, A. Castellarin, Changes in seasonality and magnitude of sub-daily rainfall extremes in Emilia-Romagna (Italy) and potential influence on regional rainfall frequency estimation, *J Hydrol Reg Stud.* 32 (2020) 100751. <https://doi.org/10.1016/J.EJRH.2020.100751>.
- [82] E. Brattich, J.A.G. Orza, P. Cristofanelli, P. Bonasoni, A. Marinoni, L. Tositti, Advection pathways at the Mt. Cimone WMO-GAW station: Seasonality, trends, and influence on

- atmospheric composition, *Atmos Environ.* 234 (2020).  
<https://doi.org/10.1016/j.atmosenv.2020.117513>.
- [83] P.K. Sen, Estimates of the Regression Coefficient Based on Kendall's Tau, *J Am Stat Assoc.* 63 (1968) 1379–1389. <https://doi.org/10.1080/01621459.1968.10480934>.
- [84] H.B. Mann, Nonparametric Tests Against Trend, *Econometrica.* 13 (1945) 245.  
<https://doi.org/10.2307/1907187>.
- [85] R.M. Hirsch, J.R. Slack, R.A. Smith, Techniques of Trend Analysis for Monthly Water Quality Data, *Water Resour Res.* 18 (1982) 107–121.
- [86] D.S. Wilks, *Statistical Methods in Atmospheric Sciences*, 2019.
- [87] Atta-ur-Rahman, M. Dawood, Spatio-statistical analysis of temperature fluctuation using Mann–Kendall and Sen's slope approach, *Clim Dyn.* 48 (2017) 783–797.  
<https://doi.org/10.1007/S00382-016-3110-Y/FIGURES/8>.
- [88] M. Gocic, S. Trajkovic, Analysis of changes in meteorological variables using Mann-Kendall and Sen's slope estimator statistical tests in Serbia, *Glob Planet Change.* 100 (2013) 172–182. <https://doi.org/10.1016/J.GLOPLACHA.2012.10.014>.
- [89] G. Yildirim, A. Rahman, Homogeneity and trend analysis of rainfall and droughts over Southeast Australia, *Natural Hazards.* 112 (2022) 1657–1683.  
<https://doi.org/10.1007/S11069-022-05243-9/TABLES/7>.
- [90] S. Salehi, M. Dehghani, S.M. Mortazavi, V.P. Singh, Trend analysis and change point detection of seasonal and annual precipitation in Iran, *International Journal of Climatology.* 40 (2020) 308–323. <https://doi.org/10.1002/JOC.6211>.
- [91] L. Pieri, P. Matzneller, N. Gaspari, I. Marotti, G. Dinelli, P. Rossi, Bulk atmospheric deposition in the southern Po Valley (Northern Italy), *Water Air Soil Pollut.* 210 (2010) 155–169. <https://doi.org/10.1007/S11270-009-0238-Y>.
- [92] L.U. Fontanella, M. Tomassetti, G. Visco, M.P. Sammartino, Characterization of Rome's rainwater in the early of 2018 aiming to find correlations between chemical-physical parameters and sources of pollution: a statistical study, *J Atmos Chem.* 78 (2021).  
<https://doi.org/10.1007/s10874-020-09409-2>.
- [93] R. Huo, L. Li, H. Chen, C.Y. Xu, J. Chen, S. Guo, Extreme Precipitation Changes in Europe from the Last Millennium to the End of the Twenty-First Century, *J Clim.* 34 (2021) 567–588. <https://doi.org/10.1175/JCLI-D-19-0879.1>.
- [94] H.M. Liljestrand, Average rainwater pH, concepts of atmospheric acidity, and buffering in open systems, *Atmospheric Environment* (1967). 19 (1985) 487–499.  
[https://doi.org/10.1016/0004-6981\(85\)90169-6](https://doi.org/10.1016/0004-6981(85)90169-6).
- [95] R. Balestrini, S. Arisci, M.C. Brizzio, R. Mosello, M. Rogora, A. Tagliaferri, Dry deposition of particles and canopy exchange: Comparison of wet, bulk and throughfall deposition at five forest sites in Italy, *Atmos Environ.* 41 (2007) 745–756.  
<https://doi.org/10.1016/J.ATMOENV.2006.09.002>.
- [96] C.H. Song, G.R. Carmichael, The aging process of naturally emitted aerosol (sea-salt and mineral aerosol) during long range transport, 1999.
- [97] X. Lu, L.Y. Li, N. Li, G. Yang, D. Luo, J. Chen, Chemical characteristics of spring rainwater of Xi'an city, NW China, *Atmos Environ.* 45 (2011) 5058–5063.  
<https://doi.org/10.1016/J.ATMOENV.2011.06.026>.
- [98] C. Gollmer, I. Höfer, M. Kaltschmitt, Additives as a fuel-oriented measure to mitigate inorganic particulate matter (PM) emissions during small-scale combustion of solid biofuels, *Biomass Convers Biorefin.* 9 (2019) 3–20. <https://doi.org/10.1007/s13399-018-0352-4>.
- [99] J. Vuorenmaa, A. Augustaitis, B. Beudert, W. Bochenek, N. Clarke, H.A. de Wit, T. Dirnböck, J. Frey, H. Hakola, S. Kleemola, J. Kobler, P. Krám, A.J. Lindroos, L. Lundin, S. Löfgren, A. Marchetto, T. Pecka, H. Schulte-Bisping, K. Skotak, A. Srybny, J. Szpikowski, L. Ukonmaanaho, M. Váňa, S. Åkerblom, M. Forsius, Long-term changes (1990–2015) in the atmospheric deposition and runoff water chemistry of sulphate, inorganic nitrogen and

acidity for forested catchments in Europe in relation to changes in emissions and hydrometeorological conditions, *Science of the Total Environment*. 625 (2018) 1129–1145. <https://doi.org/10.1016/j.scitotenv.2017.12.245>.

- [100] K. Tørseth, W. Aas, K. Breivik, A.M. Fjaeraa, M. Fiebig, A.G. Hjellbrekke, C. Lund Myhre, S. Solberg, K.E. Yttri, Introduction to the European Monitoring and Evaluation Programme (EMEP) and observed atmospheric composition change during 1972-2009, *Atmos. Chem. Phys.* 12 (2012) 5447–5481. <https://doi.org/10.5194/acp-12-5447-2012>.
- [101] European Environmental Agency, Air quality in Europe 2021 —Report no. 15/2021, 2021. <https://doi.org/10.2800/549289>.

## Tables

	Mean	Median	Min	Max	Std. Dev.
Alkalinity	0.045	0.030	0	0.71	0.065
pH	6.0	6.1	4.5	7.4	0.6
EC	21.0	17.2	4.6	123.0	13.9
Na <sup>+</sup>	20.8	16.7	0.9	196.4	18.3
NH <sub>4</sub> <sup>+</sup>	52.4	46.9	1.3	211.7	27.7
K <sup>+</sup>	4.5	3.3	0.3	44.3	4.7
Mg <sup>2+</sup>	10.4	8.5	0.6	53.1	7.4
Ca <sup>2+</sup>	56.0	37.4	4.5	753.0	68.4
Cl <sup>-</sup>	23.4	17.8	1.2	218.6	23.8
NO <sub>3</sub> <sup>-</sup>	11.5	9.9	2.9	46.2	6.4
SO <sub>4</sub> <sup>2-</sup>	40.5	33.7	5.6	221.0	28.0
PO <sub>4</sub> <sup>3-</sup>	0.25	0.15	0.01	3.2	0.34

**Table 1.** Basic statistics for experimentally determined values of pH, Alkalinity (meq/L), EC (electrical conductivity; in  $\mu\text{S/cm}$ ), and ions ( $\mu\text{eq/L}$ ) in bulk samples collected in Boschi di Carrega in the period May 1997 - December 2019. Mean is the arithmetic mean of the samples. Min = minimum; Max = maximum; Std.Dev. = standard deviation.

Variable	Mann Kendall p value	Seasonal Mann Kendall p value	Mean change per year
pH	<b>0.0007</b>	<i>0.0857</i>	+0.0200
EC	<b>0.0085</b>	<b>0.0029</b>	-0.4100
Alkalinity	0.36751	0.31565	+0.0000
NO <sub>3</sub> <sup>-</sup>	<b>0.0002</b>	<i>0.0829</i>	-0.0100
SO <sub>4</sub> <sup>2-</sup> ,	<b>0.0000</b>	<b>0.0000</b>	-0.0900
Cl <sup>-</sup>	<b>0.0286</b>	<i>0,0575</i>	-0.0100
PO <sub>4</sub> <sup>3-</sup>	0.25423	0.21824	-0.0800
NH <sub>4</sub> <sup>+</sup>	<b>0.0028</b>	<b>0.0018</b>	-0.0100
Ca <sup>2+</sup>	<b>0.0009</b>	<b>0.0009</b>	-0.0200
Mg <sup>2+</sup>	<b>0.0282</b>	0.0551	0.0000
Na <sup>+</sup>	<b>0.0171</b>	<b>0.0178</b>	-0.0100
K <sup>+</sup>	0.3303	0.8135	0.0000
N tot	<i>0.0873</i>	<b>0.0167</b>	-0.0300
NH <sub>4</sub> <sup>+</sup> /NO <sub>3</sub> <sup>-</sup>	0.1281	0.1277	0.0000
NH <sub>4</sub> <sup>+</sup> / SO <sub>4</sub> <sup>2-</sup>	<b>0.0000</b>	<b>0.0000</b>	+0.0500

**Table 2.** Results of the Mann-Kendall test and of the seasonal Kendall test for the monthly time series for the detection of monotonic trends applied on the 1997–2019 time series collected at the Boschi di Carrega sampling site. For each case, the p (significance) value and the mean change per year from the Theil-Sen slope are presented. The number is in bold when significant at the 0.05 level, in italic when the trend is only weakly significant, thus, at the 0.01 level.



# Figures

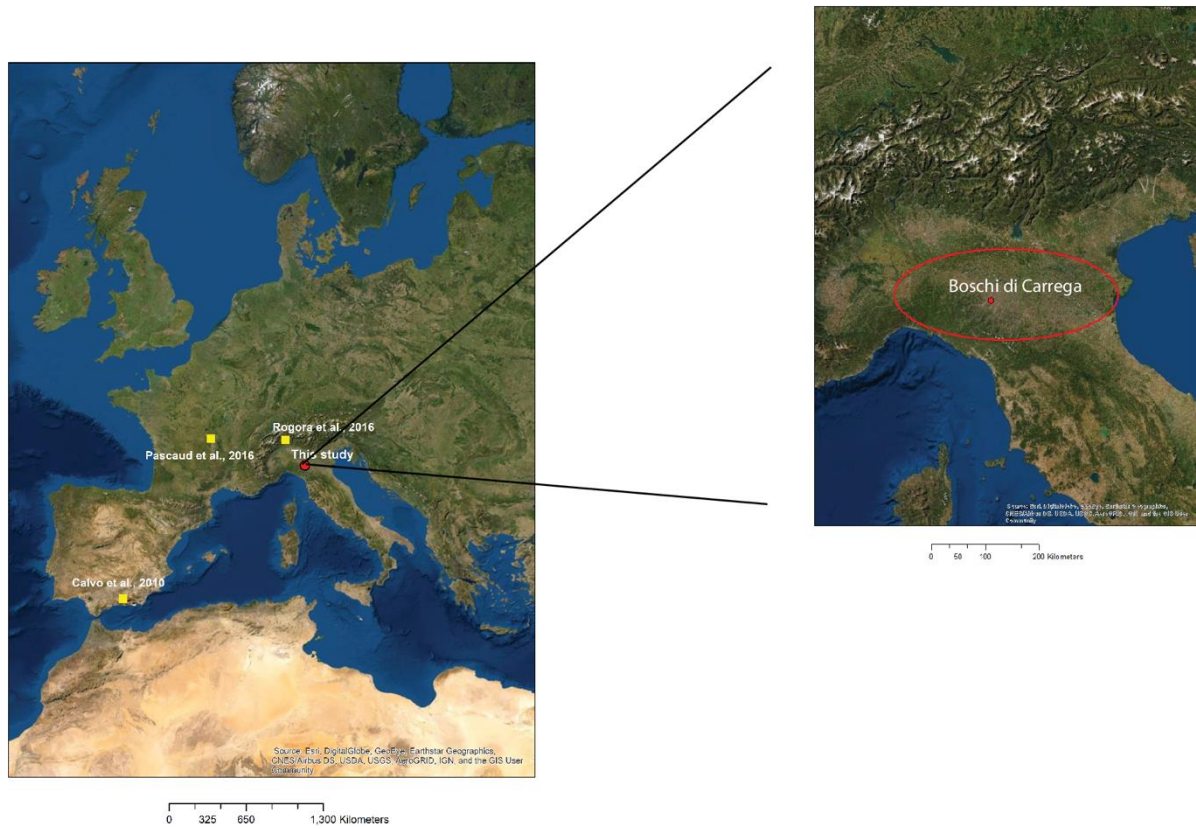


**Figure 1.** Map representing: left panel) the position of the sampling site (Boschi di Carrega, red dot) and of the other sampling sites (Lake Maggiore in Italy for Rogora et al., 2016; Granada in Spain for Calvo et al., 2010; various French sites for Pascaud et al., 2016) used to support the interpretation of the concentration ranges (yellow squares; see Section 4.4) in Europe; right panel) zoom of the sampling site (red dot) and the Po Valley (red ellipse) (source: Esri and the GIS User Community).

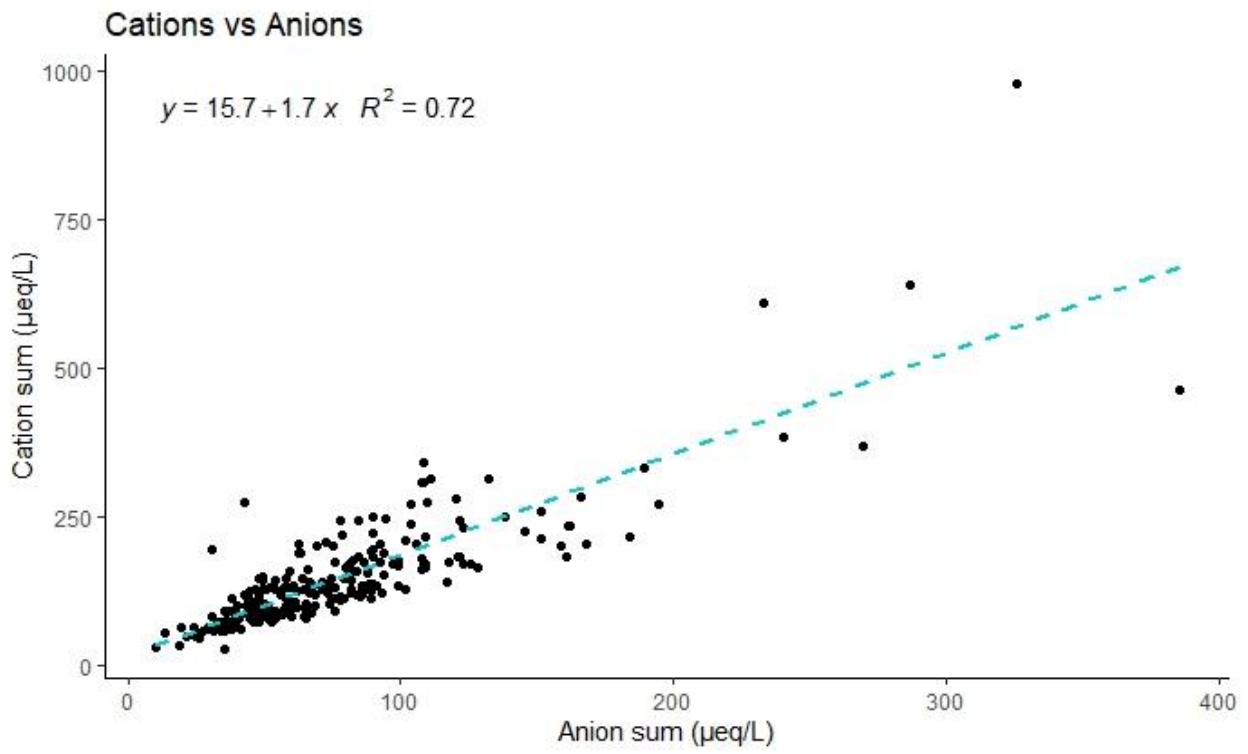


**Figure 2.** Scatter plot of cations sum vs. anions sum per month (in µeq/L) collected in Boschi di Carrega.

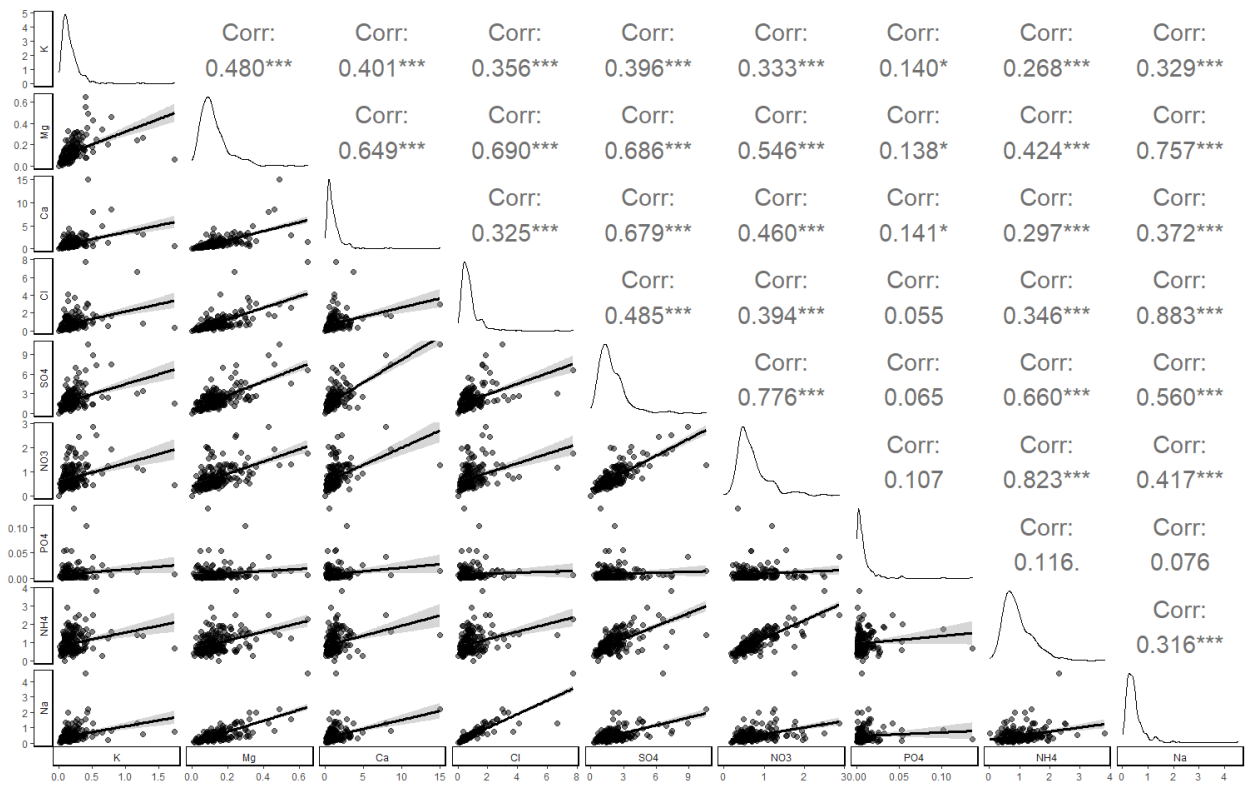


**Figure 3.** Lower panel, left from the diagonal: scatterplots of the ions (mg/l) analysed in the weekly bulk deposition samples collected in Boschi di Carrega. The diagonal shows the frequency distribution of the parameters. Upper panel, right from the diagonal: Spearman's rank correlation coefficient values for ionic composition in Boschi di Carrega from May 1997 to December 2019. The stars indicate the significance level ( $p$ ): one star stands for  $p < 1$ , two stars for  $p < 0.1$  and three stars for  $p < 0.01$ .

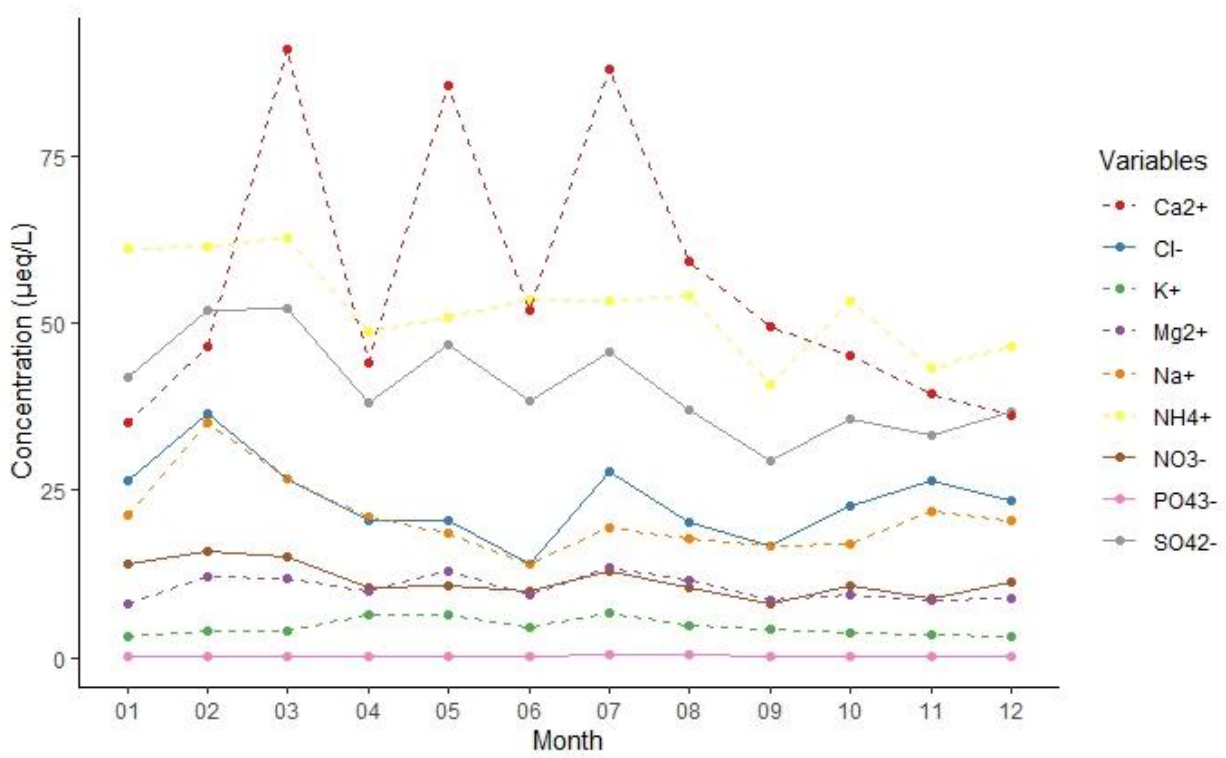


**Figure 4.** Monthly concentration of cations (with dashed line type) and anions (with solid line type) in samples of bulk deposition collected in Boschi di Carrega.

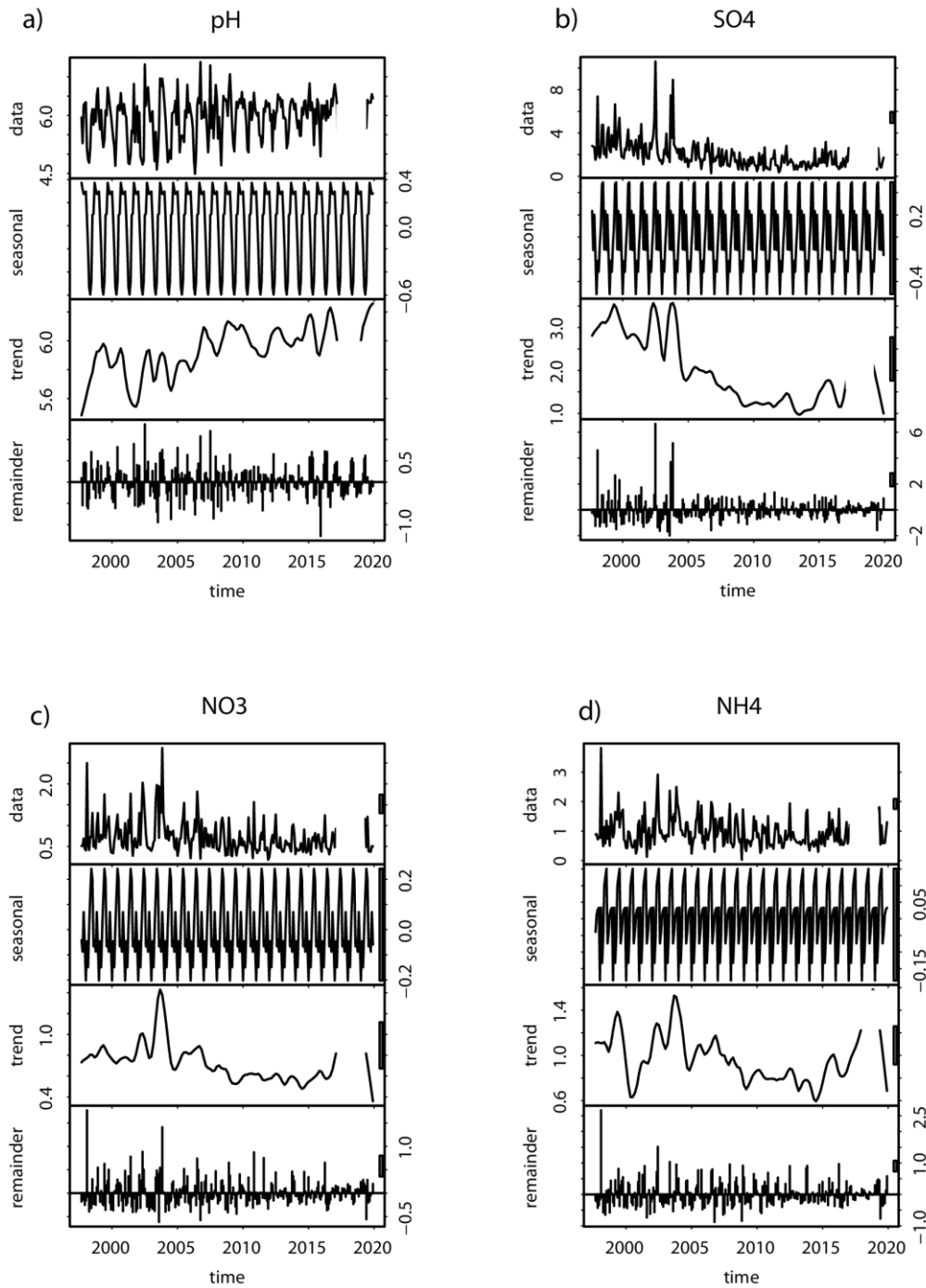


**Figure 5.** STL decomposition for the time series of: a) pH; b)  $\text{SO}_4^{2-}$ ; c)  $\text{NO}_3^-$ ; d)  $\text{NH}_4^+$ , from May 1997 to December 2019 in Boschi di Carrega. All the panels include the monthly data in the upper panel, followed by the seasonal, trend and remainder components. The concentration of the ions in the plots is in mg/L.

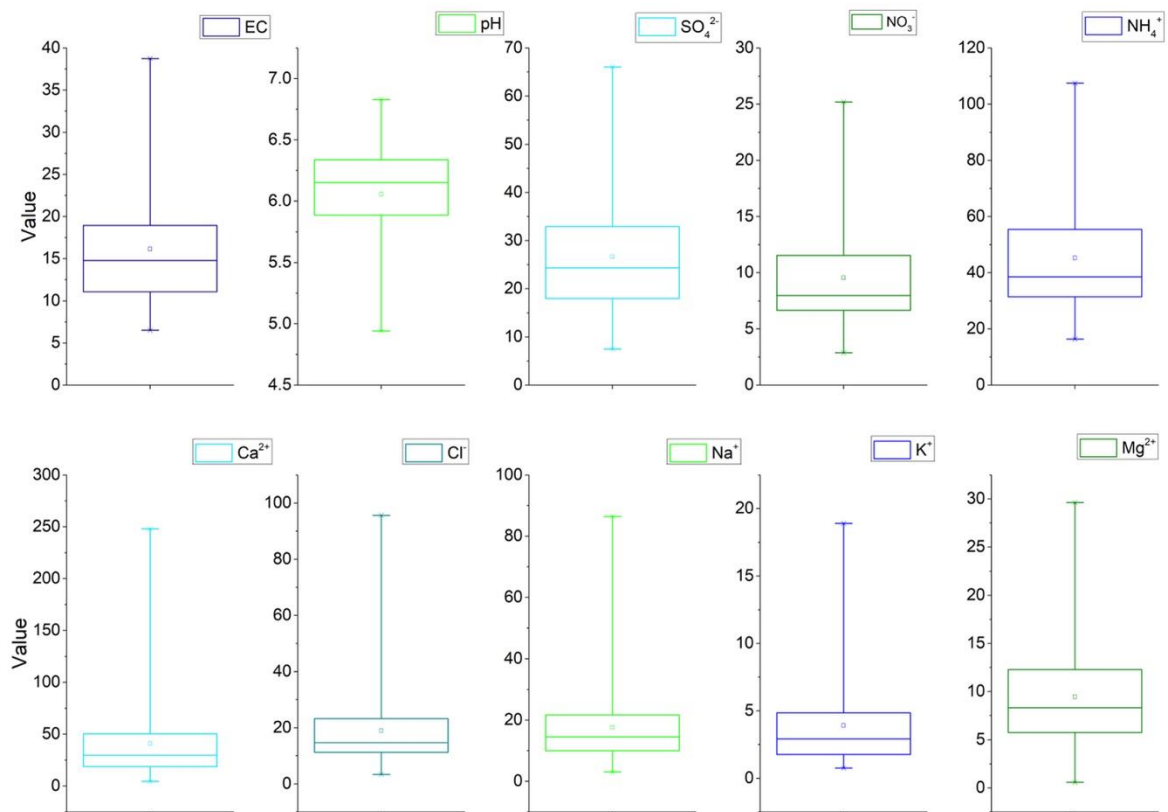


**Figure 6.** Box and whiskers plots presenting a summary for deposition composition representative for southern European sites: EC (electrical conductivity; in  $\mu\text{S}/\text{cm}$ ), pH and ions ( $\mu\text{eq}/\text{L}$ ). The box encloses the 25-75th percentile range, the line inside the box represents the median value, whereas the mean is represented by the dot. The whiskers range between the minimum and maximum values. Data used are from the last 10 years of sampling at the Boschi di Carrega site.

## Supplementary materials

### **Safeguarding outdoor cultural heritage materials in an ever-changing troposphere: challenges and new guidelines for artificial ageing test**

Andrea Timoncini<sup>a</sup>, Erika Brattich<sup>b\*</sup>, Elena Bernardi<sup>c</sup>, Cristina Chiavari<sup>a</sup>, Laura Tositti<sup>d</sup>

<sup>a</sup>Department of Cultural Heritage, University of Bologna, Via degli Ariani 1, 48121 Ravenna, Italy,

<sup>b</sup>Department of Physics and Astronomy «Augusto Righi», University of Bologna, via Irnerio 46, 40126 Bologna, Italy,

<sup>c</sup>Department of Industrial Chemistry «Toso Montanari», University of Bologna, Viale del Risorgimento 4, 40136 Bologna, Italy,

<sup>d</sup>Department of Chemistry «Giacomo Ciamician», University of Bologna, Via Selmi 2, Bologna, University of Bologna.

**Table SI1.** Summary statistics (mean, standard deviation, maximum and minimum values) of the last 10 years data of deposition composition at the Boschi di Carrega sampling site. pH, EC (electrical conductivity; in  $\mu\text{S}/\text{cm}$ ), and ions concentration ( $\mu\text{eq}/\text{L}$ ).

Site	Boschi di Carrega (Po Valley, Italy)			
Sampling period	2010-2019			
Atmospheric deposition type	Bulk			
Chemical parameter	Mean	Dev.St.	Max	Min
pH	6.1	0.1	6.8	4.9
EC	16.1	6.6	38.7	6,51
Sulfate	26.8	12.7	66.1	7.5
Nitrate	9.6	4.3	25.21	2.9
Chloride	19.0	14.3	95.6	3.4
Calcium	41.3	36.5	248.0	4.6
Potassium	3.9	3.3	18.9	0.8
Magnesium	9.5	5.6	29.6	0.6
Ammonium	45.4	19.6	107.5	16.4
Sodium	17.7	13.3	86.4	3.0